The energetic electron population dynamics at Jupiter, Saturn, Uranus and Neptune as revealed by historical spacecraft observations and physics-based models

Daniel Santos-Costa[1,1], Quentin Nénon[2,2], Emma Woodfield[3,3], Henry Garrett[4,4], Insoo Jun[4,4], and Angélica Sicard[5,5]

[1]Southwest Research Institute
[2]Research Institute in Astrophysics and Planetology
[3]British Antarctic Survey
[4]JPL/Caltech
[5]ONERA/DPHY

January 20, 2023

Abstract

We review the mechanisms that shape the spatial distributions of energetic electrons trapped in the magnetospheres of Jupiter, Saturn, Uranus and Neptune. To determine what controls the energy and spatial distributions throughout the different magnetospheres, we compute the time evolution of particle distributions with the help of a diffusion theory particle transport code that solves the governing 3-D Fokker-Planck equation. We discuss the processes already accounted for in our physics-based models of the outer planet electron radiation belts but also those suspected to be missing to improve our model results. Our theoretical modeling is guided by the analysis of particle, field and wave data collected by Pioneer 10&11 and Galileo at Jupiter, Cassini at Saturn, and during Voyager 2's flyby of Uranus in January 1986 and at Neptune in August 1989.

COSPAR 2022
44th SCIENTIFIC ASSEMBLY
16-24 July 2022, Athens, Greece
aMUSEd by the Athenian URANIA

THE ENERGETIC ELECTRON POPULATION DYNAMICS AT JUPITER, SATURN, URANUS AND NEPTUNE AS REVEALED BY HISTORICAL SPACECRAFT OBSERVATIONS AND PHYSICS-BASED MODELS

Daniel Santos-Costa[(1)], Quentin Nenon[(2)], Emma Woodfield[(3)], Henry Garrett[(4)], Insoo Jun[(4)], Angelica Sicard[(5)]
(1) Southwest Research Institute, USA (2) IRAP, France (3) BAS, UK (4) NASA/JPL (5) ONERA/DPHY, France

VIRTUAL POSTER
POSTER NUMBER
B5.2 TF-024

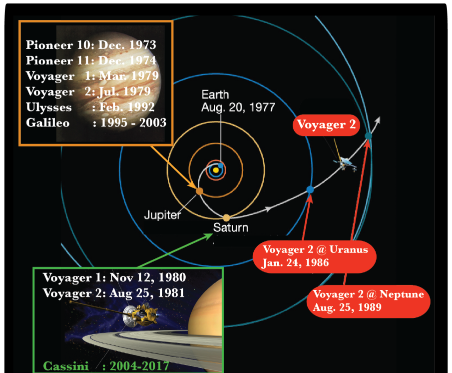

ABSTRACT

We review the mechanisms that shape the spatial distributions of energetic electrons trapped in the magnetospheres of Jupiter, Saturn, Uranus and Neptune. To determine what controls the energy and spatial distributions throughout the different magnetospheres, we compute the time evolution of particle distributions with the help of a diffusion theory particle transport code that solves the governing 3-D Fokker-Planck equation. We discuss the processes already accounted for in our physics-based models of the outer planet electron radiation belts but also those suspected to be missing to improve our model results. Our theoretical modeling is guided by the analysis of particle, field and wave data collected by Pioneer 10&11 and Galileo at Jupiter, Cassini at Saturn, and during Voyager 2's flyby of Uranus in January 1986 and at Neptune in August 1989.

DATA-BASED MODELS of OUTER PLANETS' ENERGETIC ELECTRON DISTRIBUTIONS

JPL/GIRE model

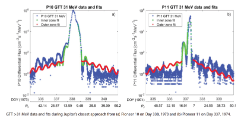

JPL/GIRE model is based on Pioneer 10/11, Voyager 1/2 and Galileo orbiter data and provides energy and pitch-angle distributions of ~0.01-100 MeV energy electrons for r < 50 Rj (after Divine & Garett, JGR, 1983; Garett & Jun, JGR 2020).

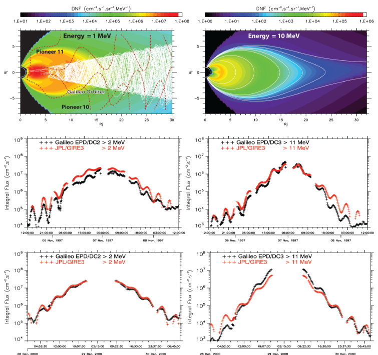

JPL/SATRAD-electron model

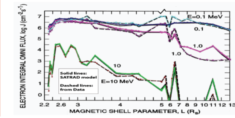

JPL/SATRAD electron model is based on Pioneer 11 & Voyager 2 data and provides energy and pitch-angle distributions of electrons with energies of ~0.04-10 MeV for L-shell = 2.3 - 13 (after Jun et al., IEEE Transactions on Plasma Sciences, 2019).

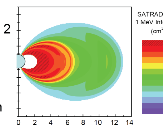

From multi-year averaged data sets (Cassini mission)

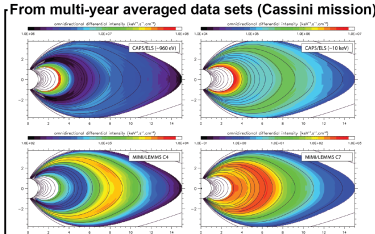

Samples of multi-year averaged data for different energy channels of CAPS/ELS and MIMI/LEMMS instruments for the period 2004-2013.

JPL/UMOD-electron model

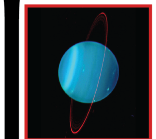

JPL/UMOD electron model is based on Voyager 2 data and provides energy and pitch-angle distributions of electrons with energies of 0.022-2.5 MeV for L-shell ~ 6 - 15 (after Jun et al., IEEE Transactions on Plasma Sciences, 2019).

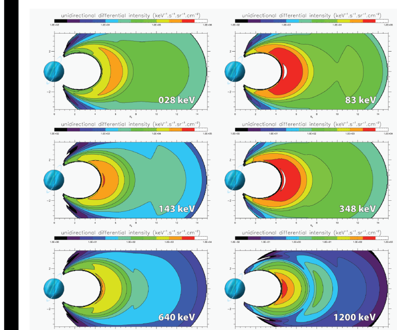

Meridian profiles of the Uranian energetic electron population inferred from in-situ data (after Mauk et al., 1987; Selesnick and Stone, 1991; Garrett et al., 2015). Note that there is an absence of data inside ~4.2 R_U that prevents to empirically model the charged particle environment close to the planet.

JPL/NMOD-electron model

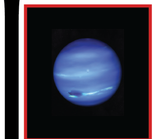

JPL/NMOD electron model is based on Voyager 2 data and provides energy and pitch-angle distributions of electrons with energies of 0.025-5 MeV for L-shell ~ 1.4 - 28 (after Jun et al., IEEE Transactions on Plasma Sciences, 2019).

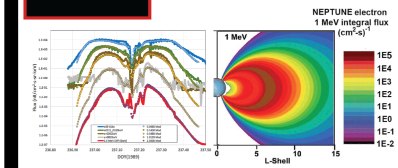

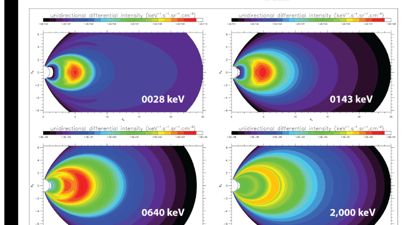

Meridian profiles of the Neptune's energetic electron population inferred from in-situ data (after Mauk et al., 1991; Stone et al., 1989; Garrett & Evans, 2017).

INSIGHTS into OUTER PLANETS' ENERGETIC ELECTRON DISTRIBUTIONS from PHYSICS-BASED MODELS

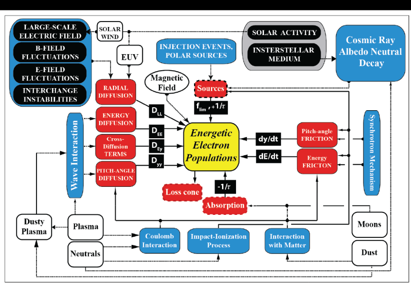

Three-dimensional distributions of electron population are calculated from numerical solutions of the governing 3-D Fokker-Planck equation

$$\begin{aligned}
\frac{\partial f}{\partial t} &= (S)-(L)+\left[\frac{1}{G}\frac{\partial G}{\partial L}D_{LL}+\frac{\partial D_{LL}}{\partial L}\right]\frac{\partial f^{\times}}{\partial L}+(D_{LL})\frac{\partial^2 f^{\times}}{\partial L^2}\\
&- \left[\frac{1}{G'}\left(\frac{\partial G'}{\partial E}\right)\left(\sum\frac{dE}{dt}\right)+\sum\frac{\partial}{\partial E}\left(\frac{dE}{dt}\right)-\frac{1}{G'}\left(\frac{\partial G'}{\partial y}\right)\left(\frac{dy}{dt}\right)-\frac{\partial}{\partial y}\left(\frac{dy}{dt}\right)\right]f^*\\
&- \left[\left(\sum\frac{dE}{dt}\right)-\frac{1}{G'}\left(\frac{\partial G'}{\partial E}\right)D_{EE}-\frac{\partial D_{EE}}{\partial E}-\frac{1}{G'}\left(\frac{\partial G'}{\partial y}\right)D_{yE}-\frac{\partial D_{yE}}{\partial y}\right]\frac{\partial f^*}{\partial E}\\
&- \left[\left(\frac{dy}{dt}\right)-\frac{1}{G'}\left(\frac{\partial G'}{\partial E}\right)D_{Ey}-\frac{\partial D_{Ey}}{\partial E}-\frac{1}{G'}\left(\frac{\partial G'}{\partial y}\right)\left(\sum D_{yy}\right)-\sum\frac{\partial D_{yy}}{\partial y}\right]\frac{\partial f^*}{\partial y}\\
&+ (D_{EE})\frac{\partial^2 f^*}{\partial E^2}+2(D_{yE})\frac{\partial^2 f^*}{\partial E\partial y}+\left(\sum D_{yy}\right)\frac{\partial^2 f^*}{\partial y^2}
\end{aligned}$$

while accounting for different source, loss, transport, diffusion and friction mechanisms (see flow chart).

	Earth	Jupiter	Saturn	Uranus	Neptune
Radius, R_{Planet} (km)	6,373	71,398	60,330	25,559	24,764
Spin Period (Hours)	24	9.9	10.7	17.2	16.1
Dipolar Magnetic Moment (G)	0.31	4.17	0.21	0.23	0.14
Dipole Tilt and Sense	+11.3°	-10.3°	-0.0°	-58.6°	-46.9°
Mean Distance from Sun (AU)	1	5.2	9.5	19	30
Solar Wind RAM pressure (nPa)	~1–4	~0.04-0.2	~0.01–0.04	~0.003–0.006	~0.001–0.003
Solar F10.7 cm Radio Flux (sfu)	~60–300	~60–300	~60–300	~60–300	~60–300
Cosmic Ray Flux ($cm^{-2}.s^{-1}$)	~<5 10^8	~<6 10^8	~1 10^8–8 10^8	~2 10^8–1 10^9	~3 10^8–2 10^9
Size of Magnetosphere	11 R_E	50–100 R_J	16–22 R_S	18 R_U	23–26 R_N
Number of Moons	1	4 ($< 5\ R_J$)	20 ($< 15\ R_S$)	18 ($< 25\ R_U$)	8 ($< 25\ R_N$)
Number of Dust Systems (Rings)	0	5 ($< 5\ R_J$)	8 ($< 15\ R_S$)	12 ($< 25\ R_U$)	10 ($< 25\ R_N$)

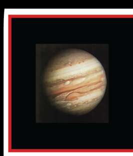

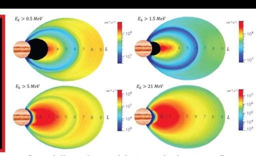

Omnidirectionnal integral electron fluxes predicted by the Salammbô model in a magnetic meridian plan (after Nenon et al., JGR 2017).

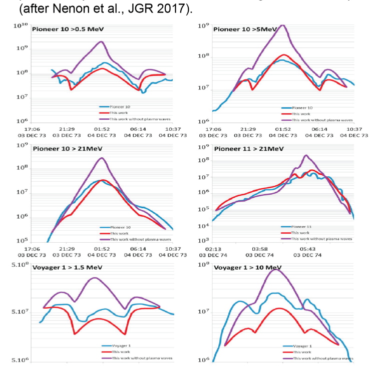

Flux predictions along the trajectories of Pioneer 10, Voyager 1, and Pioneer 11 (blue color) with (red) or without (purple) Whistler-mode chorus waves at L = 6 - 9.5. The integral omnidirectional fluxes are expressed in $cm^{-2}\ s^{-1}$ (after Nenon et al., JGR 2017).

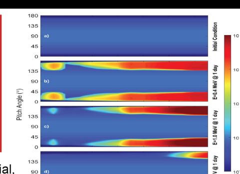

(Right) Theoretical radial, energy and angular response of electron population to Whistler mode Hiss waves (after Woodfield et al., GRL, 2022)

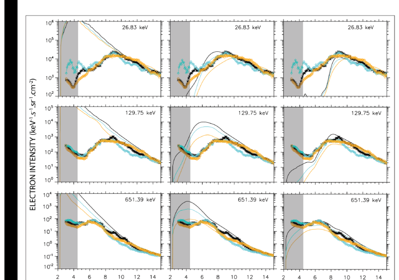

Comparisons between MIMI/LEMMS data and model when simulations include only radial transport (left-hand panels), combine radial diffusion with interaction with neutrals and a polar source (middle panels), and account for all previous mechanisms + Whistler mode Chorus wave interaction (right-hand panels). Symbols are used to display the data. Black color is used to display radial profiles for 80, cyan for 40, and orange for 20-degree pitch-angle.

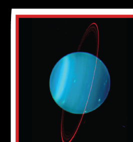

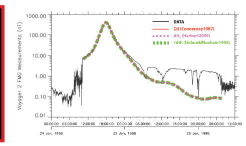

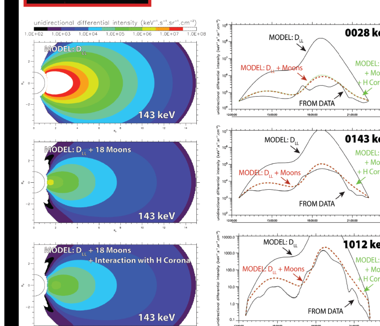

(Left set of panels) Meridian profiles of Uranian energetic electron population when model accounts only for radial diffusion (top), radial diffusion and sweeping effect by 18 moons (middle), and all previous processes + interaction with H corona (bottom). **(Right set of panels)** Data-model comparisons along Voyager 2's trajectory for different LECP energy channels. Three sets of model results are discussed for each energy: (1) Radial diffusion D_{LL}; (2) D_{LL} + sweeping effect by 18 moons; and (3) D_{LL} + sweeping effect by 18 moons + interaction with H corona.

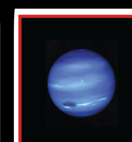

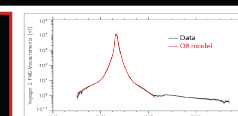

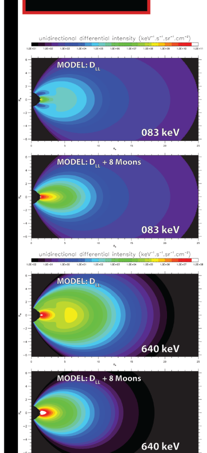

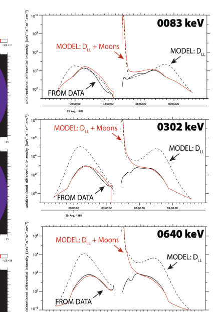

Samples of simulation results demonstrating the coupled role of radial transport and sweeping effect for different energies and L < 25. **(Left 4 panels)** Meridian profiles of Neptune's energetic electron population for 2 energies and simulation cases. **(Top 3 panels)** Data-model comparisons along Voyager 2's trajectory.